Transactions, SMiRT-22
San Francisco, California, USA - August 18-23, 2013
Division II (Fracture Mechanics)

VARIATION OF COHESIVE ZONE PARAMETERS WITH CRACK TIP STRESS TRIAXIALITY

Nevil Martin Jose[1], B. K. Dutta[1], K. K Vaze[1]

[1] Reactor Safety Division, Hall-7, BARC, Mumbai, Maharashtra, India – 400 085 (nevil@barc.gov.in)

ABSTRACT

Cohesive zone modeling (CZM) is used to simulate the initiation and propagation of cracks in solids using the finite element method. The most important step in CZM is the determination of cohesive parameters. Cohesive parameters depend not only on the material but also on the crack tip stress triaxiality. In this work, cohesive parameters are obtained as a function of crack tip stress triaxiality for SA333 Grade 6 steel and 20MnMoNi55 steel, by fitting the simulated crack extensions to the experimental data for a number of specimens and components having different crack tip stress triaxiality.

1. INTRODUCTION

Cohesive zone modeling is a damage mechanics methodology used to simulate the initiation and propagation of cracks in solids using the finite element (FE) technique. In a cohesive zone model, a narrow band of vanishing thickness termed the cohesive zone which follows a traction separation law (TSL) is assumed to exist ahead of a crack tip to represent the fracture process zone. Under external loading the atomic structure of a material changes and is reflected as the variations in cohesive traction as dictated by the traction separation law. Crack growth occurs when the separation of the cohesive surfaces reaches a critical value at which the cohesive traction vanishes. The cohesive zone modeling approach does not involve any crack tip stress singularities, and the material failure is controlled by quantities such as displacements and stresses.

SA333 Grade-6 is low carbon steel used in the PHT piping of the Indian PHWRs. 20MnMoNi55 material is a popular pressure vessel material used in many nuclear industries. Cohesive zone analysis may be used for the integrity analysis of these components. Cohesive zone modeling requires the determination of the values of TSL's parameters. Since these parameters depends not only on the material, but also on the crack tip stress triaxiality of the component to be analysed, the variation of these parameters with respect to the crack tip stress triaxiality also needs to be known.

2. MATERIAL PROPERTIES AND EXPERIMENTAL DETAILS

The SA333 grade 6 steel analysed in this work has a Young's Modulus of 203 GPa. It has yield strength of 285 MPa and Poisson's ratio 0.3. The uniaxial true stress vs. true plastic strain curve for the material is shown in Fig. 1. The experimental results utilized in this work are taken from fracture experiments conducted on 12 TPB and 11 C(T) specimens[1]; as well as that of three pipes[2] and two elbows[3]. All the C(T) and TPB specimens were side grooved for getting plane strain conditions. The experimental results used are 'Load v/s Displacement' and 'Crack growth v/s Displacement'. The C(T) specimens are subjected to tension loading. The TPB specimens are subjected to three point bending loading. The three pipes are subjected to four point bending loads. They have through wall cracks. The elbows are subjected to in-plane bending loads. The elbows are having through wall cracks at their intrados.

The 20MnMoNi55 steel analysed in this work has a Young's modulus of 210 GPa. It has yield strength of 465 MPa and Poisson's ratio 0.3. The uniaxial stress strain curve for the material is given in Fig 2. The experimental results (fracture tests conducted on a single C(T) specimen having no side grooves) used for this steel has been taken from literature [4].

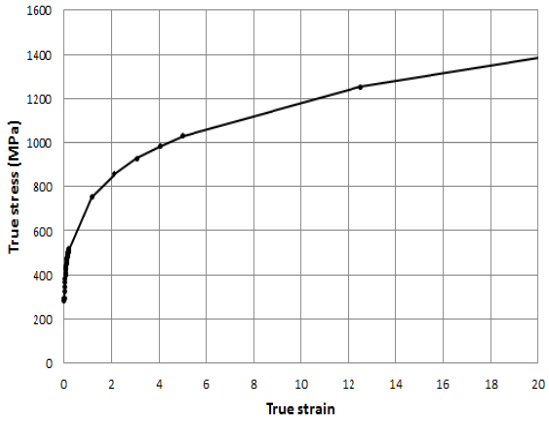

Figure 1. True stress vs. true strain for SA333 Grade 6 steel

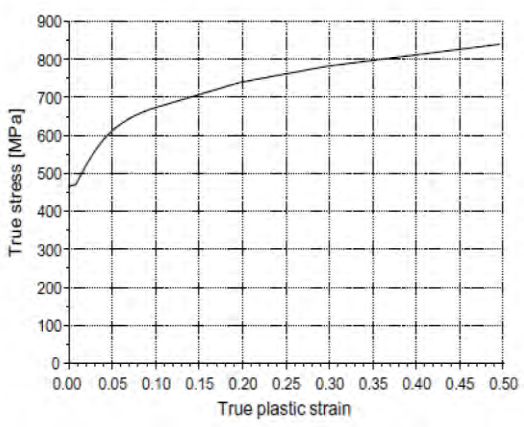

Figure 2. True stress vs. true plastic strain for 20MnMoNi55 steel [4]

3. FINITE ELEMENT MODELING OF THE C(T) AND TPB SPECIMENS

The cohesive zone finite element analysis in this work is done using the software WARP-3D. The exponential cohesive zone model available in this code is used for the purpose [5]. The finite element modeling of the C(T) and TPB specimens are done using 8-node solid brick elements. Since the specimens are having symmetries both in geometry and loading, a quarter 3D finite element mesh is used. For the specimens made of SA333 Gr. 6 steel side groove was also modeled. For the C(T) specimen made of 20MnMoNi55 steel, there is no side grove. The C(T) specimen made for 20MnMoNi55 steel has 11 layers across thickness. Layer 1 and 2 from the mid surface are of 0.2 mm and 0.3 mm respectively and the remaining 9 layers towards the side surface are of 0.5 mm thickness. The cohesive zone is modelled using 8 node cohesive elements. The behaviour of the cohesive zone is governed by the exponential cohesive law. Material and geometric non-linearity were assumed in the analysis. Material non-linearity (other than in the cohesive zone) was modelled using incremental plasticity theory with the von-Mises yield function and associated flow rule and isotropic hardening. The true stress vs. true strain curve obtained from uniaxial tension test has been used in the analysis. For the specimens made of SA333 Grade 6, cohesive elements are placed at the crack plane from the initial crack tip and up to a distance of 4 mm in the direction of crack propagation since the maximum crack growth observed during the experiments were well below 4 mm for all the TPBB and C(T) specimens taken for the analysis. For 20MnMoNi55 steel, cohesive elements were placed up to a distance of 9.6 mm. The cohesive elements used in this work employ large deformation formulation. They have a total of 8 nodes. Out of these, 4 nodes are connected to the adjacent bulk elements. These 4 nodes form the top surface of the cohesive elements. The other 4 nodes are connected to the symmetry plane. They form the bottom surface of the cohesive elements. The behavior of the cohesive elements is governed by the exponential traction separation law. The cohesive elements have an initial zero thickness. The sizes of the cohesive elements are 0.2 mm and 0.1mm in the direction of crack propagation for SA333 Grade 6 steel and 20MnMoNi55 steel, respectively. The reaction force offered by the specimen to the external applied load starts decreasing after a particular point due to crack propagation. This situation cannot be simulated by force controlled loading. So, displacement controlled loading was used for the simulations. The finite element mesh made for a TPB specimen is shown in Fig. 3 and Fig. 4.

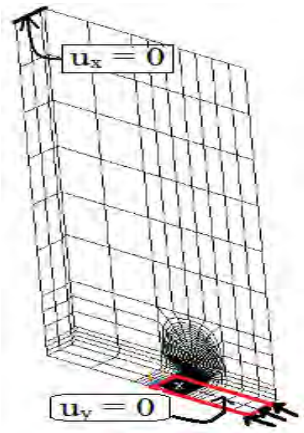

Figure 3. Quarter 3D FE mesh of the TPB specimen showing applied boundary conditions

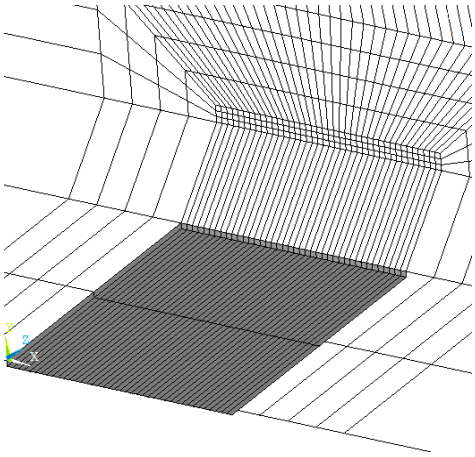

Figure 4. Enlarged view of the crack tip region of the TPB specimen showing cohesive elements (grey colored elements).

4. FINITE ELEMENT MODELING OF PIPE AND ELBOW SPECIMENS

The cohesive analyses of the pipes and elbows are also done using 8-node solid brick elements. The pipes are subjected to four point bending loads. The elbows are subjected to opening bending moments. The specimens are having symmetry in both loading and geometry. So, only 1/4th of the pipe and elbow specimens are to be modeled. The crack is simulated using constraints applied along the crack plane in the axial direction. Displacement controlled loading is applied to simulate the experimental conditions.

In the FE model, cohesive elements are placed along the crack plane from the initial crack tip up to a distance of 76.8 mm along the circumference. The maximum crack growth observed during experiments for all the pipes and elbows were well below 70 mm. The crack growth reported for the pipe and elbow specimens in the experiments were measured from their side surface. So in the analyses also, at any load step, the crack growth was calculated by counting the number of cohesive elements that got 'killed' at the side surface, up to that load step. The behavior of cohesive elements are similar to the case of C(T) and TPB specimens mentioned earlier. The size of each cohesive element in the direction of crack propagation is 0.4 mm. So, the minimum crack growth that can be simulated is 0.4 mm only.

Large strain, large displacement relations based on geometry changes are assumed in the analysis. Non-linear material behaviour of SA333 Grade-6 steel is modelled by incremental plasticity theory with von-Mises yield function, associated flow rule and isotropic hardening. The true stress - true strain curve obtained from a uni-axial tension test is used in the analysis. The finite element mesh made for the pipe and elbows are shown in Fig. 5 through Fig. 8.

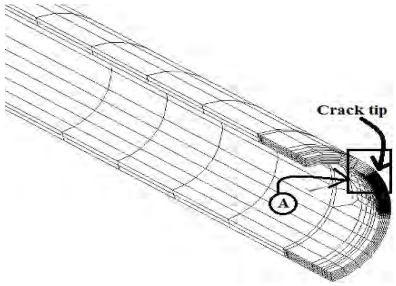

Figure. 5. Quarter 3D FE mesh for the pipe

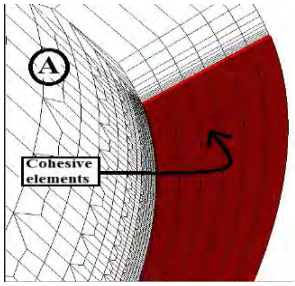

Figure.6. Enlarged view of the crack tip region (region 'A' in Fig. 5)

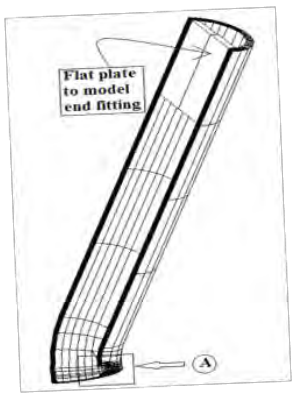

Figure. 7. Quarter 3D FE mesh for elbow

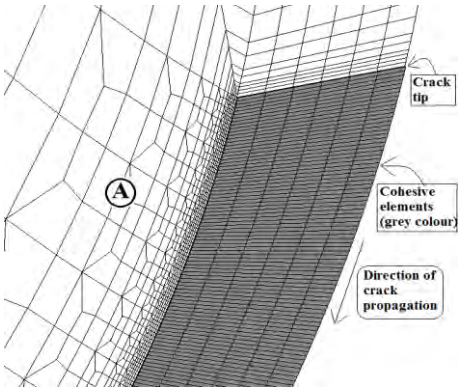

Figure 8. Enlarged view of the crack tip region of the elbow (Region 'A' in Fig. 7)

In the case of elbows, to simulate the experimental situations, a straight pipe is modeled and attached tangentially to the elbow as shown in Fig. 7. Towards the end of the pipe a flat plate is modeled to simulate the end fitting in the experiment.

5. DETERMINATION OF COHESIVE ZONE PARAMETERS FOR C(T), TPB, PIPE AND ELBOW SPECIMENS MADE OF SA333 GRADE-6 STEEL

The cohesive parameters for the C(T), TPB Pipe and Elbow specimens specimens were found by fitting the simulated results with the experimental results. The cohesive zone parameters for the exponential TSL used in this work are peak stress and fracture energy. Peak stress determines the maximum stress developed in the cohesive zone, while fracture energy determines the amount of energy required for the separation of unit area of the cohesive surface. First, a trial value for the cohesive zone parameters peak stress (equal to 3 to 4 times the yield strength) and fracture energy (equal to value of J integral at the stretch zone width from experiments conducted on the specimen) is taken and then it is varied to match with the experimental results in further analyses. The initiation of crack growth in the analyses w.r.t the applied loading depends on the value of the fracture energy (Lower the value of fracture energy earlier the crack initiation). The crack propagation rate w.r.t the applied loading depends mainly on the value of peak stress (Lower the value of peak stress, faster the crack growth). First the value of fracture energy is found out which simulates the initiation of crack growth in accordance with the experiment. Then the value of peak stress is found out which simulates the crack propagation rate in accordance with the experiment. Thus the suitable combination of peak stress and fracture energy for the given specimen is arrived at through a trial and error method. The crack growth reported for the specimens in the experiments were measured at their side surface. So in the simulation also, the crack propagation was calculated w.r.t the cohesive elements near to the side surface (cohesive elements in the layer adjacent to the side groove). The results of the cohesive zone analysis and the cohesive zone parameters obtained for a TPB specimen named T08_2C analysed in this work is shown in Fig. 9 and Fig. 10. Fig. 9 shows the fitting of the load v/s CMOD (crack mouth opening displacement) plots simulated using the cohesive zone analysis to the experimental result. Two sets of cohesive zone analysis are shown in Fig. 9, each with a different set of cohesive zone parameters. Fig. 10 shows the fitting of crack growth v/s CMOD plots simulated using cohesive zone analysis with the experimental results, for the same specimen. In these figures, the cohesive zone parameter fracture energy is denoted by G (N/mm) and the parameter peak stress by T (MPa). By comparing these two figures, the set of cohesive parameters which best simulates the experimental results are with G = 120 KJ/m^2 and T = 1540 MPa. In the similar way, the best suitable cohesive parameters for all the specimens analysed in this work are found out.

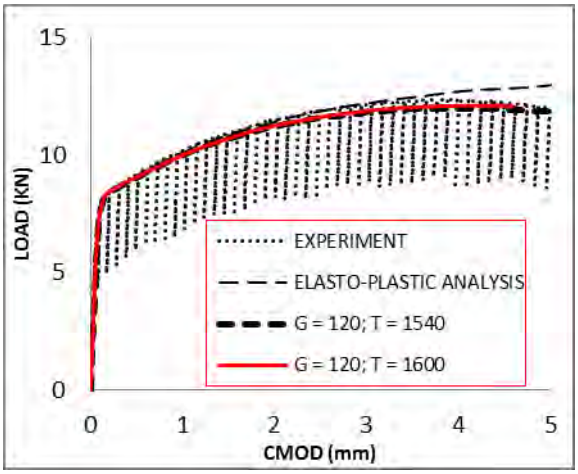

Fig. 9. Load vs. CMOD for TPB specimen T08_2C

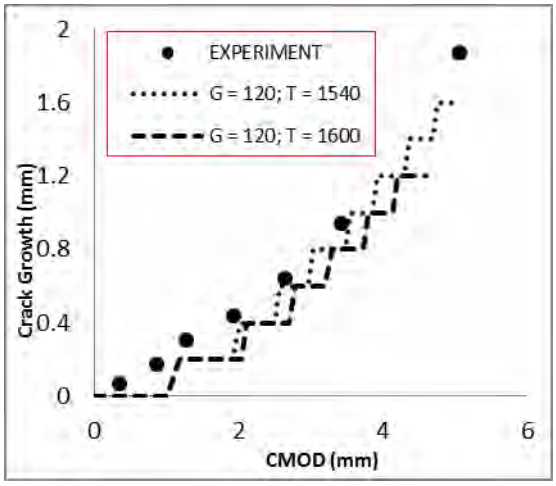

Fig. 10. Crack growth vs. CMOD for TPB specimen T08_2C

6. DETERMINATION OF THE VARIATION OF COHESIVE ZONE PARAMETERS WITH RESPECT TO THE CONSTRAINT FOR SA333 Gr 6 STEEL

The cohesive parameters determined for C(T), TPBB, pipe and elbow specimens described in the earlier sections varies with the a/W ratio, size and geometry of the specimens, even though they are made of the same material viz., SA333 Grade – 6 steel. This is so, because the fracture process in a material depends on the state of stress triaxiality at the location of the crack. The geometry, size, a/W ratio etc., in a specimen determines the state of stress triaxiality of the specimen near the crack tip. So, when these factors are different, the cohesive parameters which simulate the fracture process in cohesive zone analyses will also be different. So, the variation of cohesive parameters w.r.t crack tip stress triaxiality needs to be obtained. In this work, this is done by obtaining crack tip stress triaxiality for all specimens analysed in this work. The stress triaxiality has been quantified using the triaxiality parameter 'q' corresponding to a *J* integral value of ~210 KJ/m^2. The parameter 'q' is defined as,

$$q = (1/\sqrt{3})X(\sigma_v/\sigma_h) \quad (1)$$

where, σ_v = von-Mises equivalent stress and σ_h = hydrostatic stress. As per the definition of 'q' a low value implies a higher constraint level. The triaxiality parameter 'q' has been found out by conducting elasto-plastic finite element analysis (without any cohesive elements) considering a stationary crack. The analysis is done using the finite element code 'WARP 3D'. The analyses have large strain, large displacement assumptions. Non-linear material behaviour of SA333 Grade-6 steel is modelled by incremental plasticity theory with von-Mises yield function, associated flow rule and isotropic hardening. The true stress - true strain curve obtained from a uni-axial tension test is given as the input to the material model. The 'q' parameter is calculated on the 'fine elements' adjacent to the crack tip which lie on the crack plane. The minimum value of 'q' obtained for a specimen is taken as the constraint level in that specimen. A plot of the 'q' parameter thus calculated for a TPB specimen analysed in this work is shown in Fig. 11. The 'q' parameter value for a specimen will change with respect to the applied loading. So to compare 'q' for different specimens it should be quantified with reference to a parameter which can quantify the amount of loading applied to the specimen. The parameter suitable for quantifying the applied loading is the *J* integral. So the 'q' parameter for all the specimens are calculated when the applied *J* integral in the specimens reach a pre-defined value. This predefined value is selected randomly. The value of *J* integral selected here for this purpose is ~210 KJ/m^2. The J integral has been calculated using the standard formulas available in the literature.

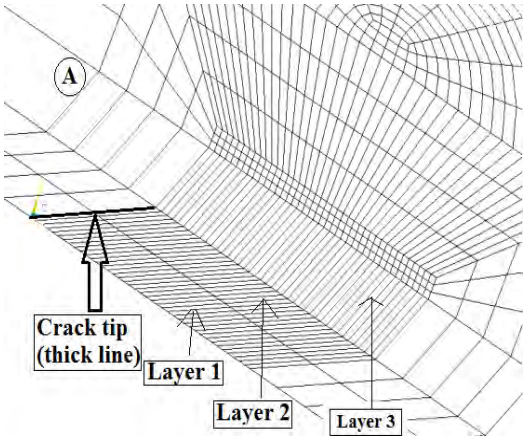

Figure. 11 a. Magnified view of the crack tip region of the FE mesh of a TPB specimen named T08_2C

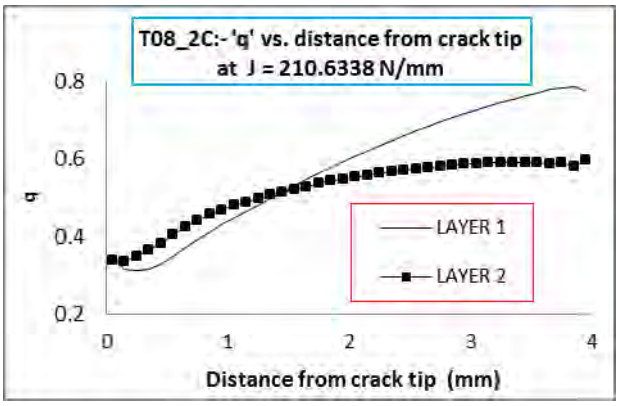

Figure 11 b. 'q' vs. distance from crack front for T08_2C. Minimum value of 'q' is obtained in layer 1 and is equal to 0.3129

The 'q' parameters obtained as explained above, for all the specimens are plotted in Fig. 12 against the value of the cohesive parameter obtained for each of these specimens. The cohesive parameter fracture energy (G) was found to be almost the same for all the specimens. However the parameter peak stress showed significant variation between specimens. So in Fig. 12 only 'q' v/s peak stress is shown. Table 1 and 2 lists 'q' values and cohesive parameters obtained for all the specimens.

Table 1:- Cohesive parameters determined for C(T), TPBB, pipe and elbow specimens. Also, the value of 'q' parameter at an applied J~210 KJ/m^2 is given for these specimens.

Sl.No:	Specimen name	Specimen Type	Thickness, B (mm)	a/W	q	G (N/mm)	T (Mpa)
1	T08_2C	TPB	8	0.305	0.3129	120	1540
2	T08_3A	TPB	8	0.347	0.310301	120	1480
3	T08_3B	TPB	8	0.356	0.311718	120	1480
4	T08_3C	TPB	8	0.333	0.306998	120	1520
5	T08_5A	TPB	8	0.511	0.305064	120	1480
6	T08_5B	TPB	8	0.513	0.304815	115	1540
7	T08_5C	TPB	8	0.442	0.303693	120	1500
8	T12_3A	TPB	12	0.362	0.28075	120	1800
9	T12_3B	TPB	12	0.354	0.283194	120	1800
10	T12_5A	TPB	12	0.507	0.259754	120	1800
11	T12_5B	TPB	12	0.505	0.258938	120	1800
12	T12_5C	TPB	12	0.43	0.273244	120	1800
13	C08_3A	C(T)	8	0.341	0.279036	120	1450
14	C08_3B	C(T)	8	0.393	0.31107	120	1560

15	C08_3C	C(T)	8	0.441	0.317579	120	1540
16	C08_5A	C(T)	8	0.49	0.31516	120	1600
17	C08_5B	C(T)	8	0.534	0.31313	120	1560
18	C08_5C	C(T)	8	0.595	0.305715	120	1520
19	C12_3A	C(T)	12	0.343	0.270773	120	1700
20	C12_3C	C(T)	12	0.446	0.275768	140	1700
21	C12_5A	C(T)	12	0.493	0.270555	120	1800
22	C12_5B	C(T)	12	0.418	0.27736	115	1800
23	C12_5C	C(T)	12	0.598	0.25094	120	1700

Table 2. Cohesive parameters determined for pipe and elbow specimens having through wall cracks. Also, the value of 'q' parameter at an applied J~210 KJ/m^2 is given for these specimens.

Sl.No:	Specimen name	Specimen Type	NB (mm)	Crack length	q	G (N/mm)	T (Mpa)
1	SPBMTWC8-1	Straight Pipe	200	65.6°	0.323739	110	1400
2	SPBMTWC8-2	Straight Pipe	200	93.9°	0.316409	120	1300
3	SPBMTWC8-3	Straight Pipe	200	126.4°	0.309682	120	1400
4	ELTWIN8-1	Elbow, Crack at intrados	200	94.96°	0.303155	120	1500
5	ELTWIN8-2	Elbow, Crack at intrados	200	125.16°	0.299091	120	1600

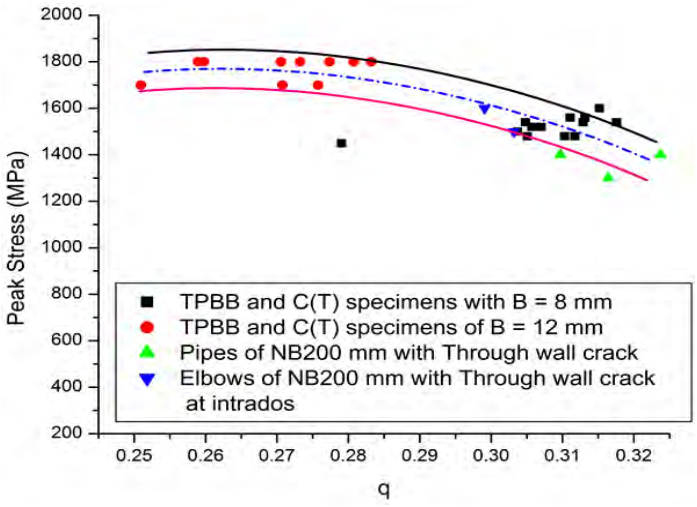

Figure 12. Plot of 'q' v/s T for specimens made of SA333 Grade 6 steel analysed in this work.

Fig. 12 shows that the the value of T increases with decreasing value of 'q'. The upper bound curve shown in the figure has been drawn by considering the uppermost values of T while the lower bound curves have been drawn by following the lowermost values of T. The middle curve is drawn parallel to both upper and bottom curves. It is seen that all the values of T obtained, except one, lie in between these upper and lower bound curves. It is also seen from the plot that as the value of 'q' decreases, the curves become more and more horizontal implying that the value of T gets saturated as the crack tip constraint increases.

7. DETERMINATION OF COHESIVE ZONE PARAMETERS FOR THE C(T) SPECIMEN MADE OF 20MnMoNi55 STEEL

The cohesive zone parameters for the C(T) specimen made of 20MnMoNi55 steel is obtained by fitting the simulated results with the experimental results, in the same way as is done for specimens made of SA333 Gr. 6. The experimental results [4] for 20MnMoNi55 consist of load v/s displacement and crack growth across the thickness at a given displacement. For this C(T) specimen, to simulate the crack across the thickness, the cohesive zone parameters had to be varied across the thickness. The FE model made for the C(T) specimen has 11 layers across the thickness. For each layer, a suitable set of cohesive zone parameters were obtained which best simulated the crack growth corresponding to that layer's position along the thickness. The cohesive zone parameters obtained for the specimen is given in Table 3. The simulated crack propagation using these parameters is shown in Fig 13. The figure also shows the corresponding experimental results. The corresponding load v/s displacement plot is shown in Fig 14.

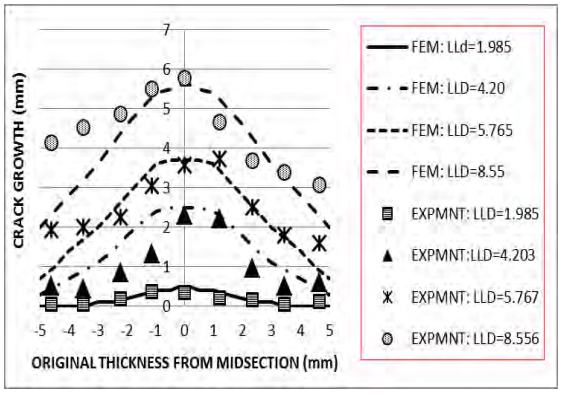

Figure 13. Crack growth simulated at different Load Line Displacement (LLD) corresponding to cohesive parameters given in Table 3.

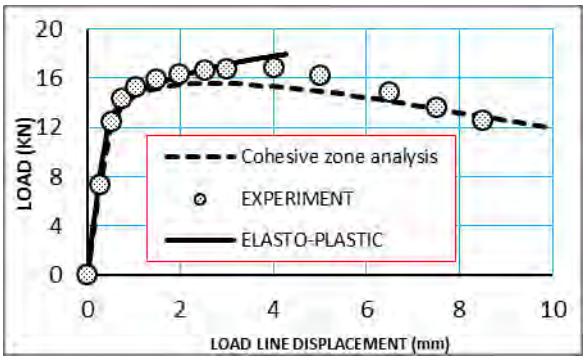

Figure 14. Load vs. displacement for the C(T) specimen made of 20MnMoNi55 steel.

8. DETERMINATION OF THE VARIATION OF COHESIVE ZONE PARAMETERS WITH RESPECT TO THE CONSTRAINT LEVEL FOR 20MnMoNi55 STEEL

The variation of cohesive parameters w.r.t stress triaxiality for 20MnMoNi55 steel was obtained in the same way for SA333 Gr. 6. Since the C(T) specimen analysed has no side groves, the constraint level varied from mid-section to the side surface. For all the 11 layers of the FE model, the triaxiality quotient 'q' was quantified. Fig 15 shows the variation of the cohesive parameter, T (peak stress) with triaxiality for 20MnMoNi55 steel. The cohesive parameter G (fracture energy) obtained was same for all the layers (i.e., G did not varied across the thickness). Table 3 lists the 'q' values obtained for all the 11 layers.

Table 3. The minimum value of 'q' parameter across different layers and the corresponding cohesive parameters for the C(T) specimen made of 20MnMoNi55. The 'q' parameter is calculated using results obtained from elasto-plastic FEA. The cohesive parameters are obtained by conducting cohesive zone analyses, as explained in previous sections.

Layer No. (starting from midsection)	The triaxiality parameter, q (at $J_{applied}$= 210.5682 N/mm)	Peak Stress (MPa)	Fracture Energy (N/mm)
1	0.294464	1480	130
2	0.294906	1480	130
3	0.297397	1480	130
4	0.301997	1480	130
5	0.30867	1480	130
6	0.320231	1480	130
7	0.333248	1480	130
8	0.353629	1342	130
9	0.384063	1205	130
10	0.414897	1067.5	130
11	0.540027	930	130

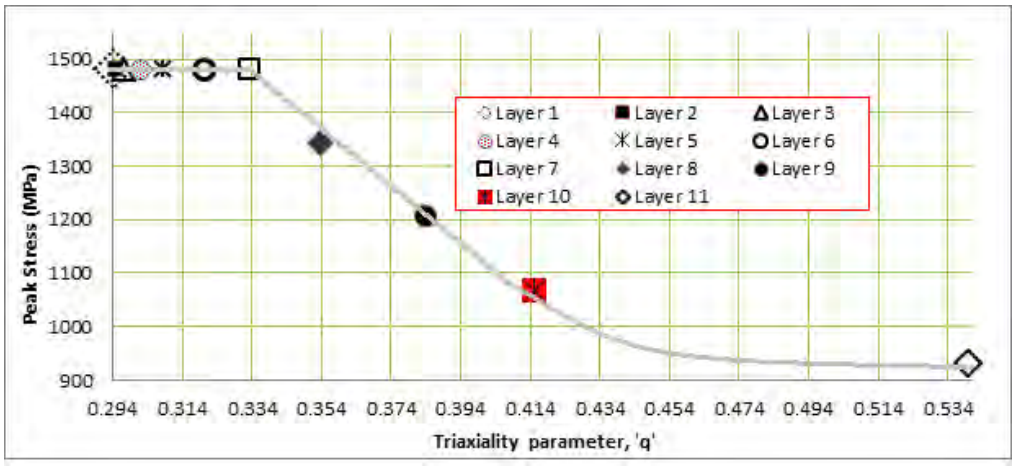

Figure 15: Plot showing 'q' vs. peak stress for 20MnMoNi55 steel obtained by conducting elastic-plastic FEA (without any cohesive elements) on the C(T) specimen.

The plot of 'q' vs. peak stress in Fig. 15 shows that to better simulate the experimental results, a higher value of peak stress (T) should be input in regions (mid-section) where stress triaxiality is high. Similarly, a smaller value of peak stress is required for regions having a low triaxiality. However, the value of fracture energy (G) is found to be independent of stress triaxiality from this analysis. Fig. 15 also shows that as the constraint level increases, the peak stress value tends to saturate.

9. CONCLUSION

1) The cohesive zone parameters for exponential traction separation law are not only material properties but also depend on the constraint level in the specimen. The cohesive parameter

fracture energy does not show appreciable variation for a given material but the parameter peak stress shows significant variation w.r.t triaxiality.

2) For a specimen with a higher value of stress triaxiality, the value of peak stress needs to be more than that for a specimen with a low value of stress triaxiality to the simulate the experimental crack growth.
3) The initiation of crack growth w.r.t the applied loading in the simulation is primarily determined by the value of fracture energy (G) used in the simulation. Lower the value of fracture energy earlier will be the initiation of crack growth and vice versa.
4) The rate of crack growth with loading is primarily determined by the value of peak stress (T). Lower the value of peak stress more will be the rate of crack growth and vice versa.
5) From the plot of 'q' vs. peak stress obtained for SA333 Grade 6 and 20MnMoNi55 steels, it was found that, the value of peak stress saturates as the constraint level increases.

REFERENCES

[1] *Specimen Size and Constraint Effects on J-R curves of SA333 Gr.6 Steel, TPB and C(T) geometries:* National Metallurgical Laboratory, Jamshedpur, India; March 2000, Project No: CIEP/98/0055

[2] J. Chattopadhyay, T.V. Pavankumar, B.K. Dutta, H.S. Kushwaha. *Experimental and analytical study of three point bend specimen and through wall circumferentially cracked straight pipe:* International Journal of Pressure Vessels and Piping 77 (2000) 455–471.

[3] J. Chattopadhyay, T.V. Pavankumar, B.K. Dutta, H.S. Kushwaha. *Fracture experiments on through wall cracked elbows under in-plane bending moment: Test results and theoretical/numerical analyses:* Engineering Fracture Mechanics 72 (2005) 1461–1497.

[4].C.R. Chen, O. Kolednik, J. Heerens, F.D. Fischer. *Three-dimensional modeling of ductile crack growth: Cohesive zone parameters and crack tip triaxiality:* Engineering Fracture Mechanics 72 (2005) 2072–2094.

[5] WARP 3D Manual (version: 16.3.2)